

Synthesis of Layered Inorganic–Organic Nanocomposite Films from Mono-, Di-, and Trimethoxy(alkyl)silane–Tetramethoxysilane Systems

Atsushi Shimojima,[†] Noritaka Umeda,[†] and Kazuyuki Kuroda^{*,†,‡}

Department of Applied Chemistry, Waseda University, Ohkubo-3, Shinjuku-ku, Tokyo 169-8555, Japan, and Kagami Memorial Laboratory for Materials Science and Technology, Waseda University, Nishiwaseda-2, Shinjuku-ku, Tokyo 169-0051, Japan

Received February 1, 2001. Revised Manuscript Received April 27, 2001

Transparent thin films of layered inorganic–organic nanocomposites were prepared by the sol–gel reactions of alkyl dimethylmethoxysilane, alkyl methyl dimethoxysilane, and alkyl trimethoxysilane in the presence of tetramethoxysilane followed by spin-coating. The macroscopic homogeneity and the nanostructural ordering of the films were strongly affected by the degree of polycondensation in the precursor solutions. The formation of siloxane networks containing organosiloxane units was confirmed by ²⁹Si MAS NMR, suggesting that the structure of the inorganic–organic interface can be designed at a molecular level by the functionalities in the alkyl methoxysilanes used. On the other hand, the ²⁹Si NMR spectra of the precursor solutions showed that the monomeric species almost disappeared and that co-condensed oligomers were formed at the initial stages of the reactions. In the cases of mono- and dimethoxysilanes, the ability to form ordered structures depends largely on the co-condensation with tetramethoxysilane in the precursor solutions.

Introduction

The construction of inorganic–organic nanocomposites with organized nanostructures is an area of extensive research in materials chemistry. The multilayered inorganic–organic thin films are one of the most important systems because they are expected to exhibit unique properties arising from structural anisotropy and compositional varieties.^{1–6} Self-assembly of trifunctional organosilanes (RSiX₃, X = Cl or OR') provides an efficient route to produce highly ordered organosiloxane monolayers in which siloxane layers and organic moieties are linked by stable Si–C bonds.⁶ However, this process normally occurs at the solid–liquid or liquid–vapor interfaces, and the formation of multilayers often requires the sequential adsorptions of monolayers containing terminal functional groups. Therefore, simple and versatile methods for the preparation of organosiloxane multilayers are of significant interest from both scientific and practical points of view.

The sol–gel processing has been developed as a practically useful way to produce inorganic–organic

nanocomposite materials.^{7,8} A variety of alkoxysilanes can be used, usually in combination with other alkoxysilanes, to form silica-based materials with desired compositions, morphologies, and properties. Recent research focuses on structural control on a nanometer-length scale. The sol–gel reaction in the presence of surfactant assemblies as structural directors is a well-known technique by which materials with various nanostructures are obtained.^{9–15} In contrast, several reports have shown the spontaneous formation of multilayered aggregates based on the self-assembly of hydrolyzed organotrialkoxysilanes.^{16–20} This process may lead to the production of a novel class of layered

* To whom correspondence should be addressed. Phone and fax: +81-3-5286-3199. E-mail: kuroda@mn.waseda.ac.jp.

[†] Department of Applied Chemistry.

[‡] Kagami Memorial Laboratory for Materials Science and Technology.

(1) Yang, H. C.; Aoki, K.; Hong, H.-G.; Sackett, D. D.; Arendt, M. F.; Yau, S.-L.; Bell, C. M.; Mallouk, T. E. *J. Am. Chem. Soc.* **1993**, *115*, 11855.

(2) Katz, H. E. *Chem. Mater.* **1994**, *6*, 2227.

(3) Marks, T. J.; Ratner, M. A. *Angew. Chem., Int. Ed. Engl.* **1995**, *34*, 155.

(4) Kimizuka, N.; Kunitake, T. *Adv. Mater.* **1996**, *8*, 89.

(5) Rouse, J. H.; MacNeill, B. A.; Ferguson, G. S. *Chem. Mater.* **2000**, *12*, 2502.

(6) Ulman, A. *Chem. Rev.* **1996**, *96*, 1533.

(7) Brinker, C. J.; Sherer, G. W. *Sol–Gel Science*; Academic Press: San Diego, CA, 1990.

(8) Wen, J.; Wilkes, G. L. *Chem. Mater.* **1996**, *8*, 1667.

(9) Sakata, K.; Kunitake, T. *J. Chem. Soc., Chem. Commun.* **1990**, 504.

(10) Ogawa, M. *J. Am. Chem. Soc.* **1994**, *116*, 7941.

(11) Lu, Y.; Ganguli, R.; Drewien, C. A.; Anderson, M. T.; Brinker, C. J.; Hong, W.; Guo, Y.; Soyey, H.; Dunn, B.; Huang, M. H.; Zink, J. I. *Nature* **1997**, *389*, 364.

(12) Brinker, C. J.; Lu, Y.; Sellinger, A.; Fan, H. *Adv. Mater.* **1999**, *11*, 579.

(13) Stein, A.; Melde, B. J.; Schroden, R. C. *Adv. Mater.* **2000**, *12*, 1403.

(14) Lu, Y.; Fan, H.; Doke, N.; Loy, D. A.; Assink, R. A.; LaVan, D. A.; Brinker, C. J. *J. Am. Chem. Soc.* **2000**, *122*, 5258.

(15) Grosso, D.; Balkenende, A. R.; Albouy, P. A.; Lavergne, M.; Mazerolles, L.; Babonneau, F. *J. Mater. Chem.* **2000**, *10*, 2085.

(16) Fukushima, Y.; Tani, M. *J. Chem. Soc., Chem. Commun.* **1995**, 241.

(17) Huo, Q.; Margolese, D. I.; Stucky, G. D. *Chem. Mater.* **1996**, *8*, 1147.

(18) Shimojima, A.; Sugahara, Y.; Kuroda, K. *Bull. Chem. Soc. Jpn.* **1997**, *70*, 2847.

(19) Ukrainczk, L.; Bellman, R. A.; Anderson, A. B. *J. Phys. Chem. B* **1997**, *101*, 531.

(20) Whilton, N. T.; Burkett, S. L.; Mann, S. *J. Mater. Chem.* **1998**, *8*, 1927.

nanocomposites with well-designed architectures that cannot be attained by using surfactant assemblies.

We have recently demonstrated a novel approach that involves the cohydrolysis and polycondensation of alkyltrialkoxysilane and tetraalkoxysilane mixtures to form transparent thin films of multilayered nanocomposites.²¹ The molecular design of the starting organoalkoxysilane plays a key role in extending this synthetic approach for the development of new materials. In particular, mono- and difunctional organosilanes, containing additional organic groups via Si–C bonds, are promising candidates because they are potentially applicable for the design and construction of organized materials with a variety of interfacial structures and organic functionalities. Although these molecules are widely utilized for the surface modification of inorganic solids, simple sol–gel reactions only result in the formation of either oligomers or one-dimensional polymers due to their poor cross-linking abilities. It is expected that the co-condensation with tetraalkoxysilane will overcome this limitation and enable us to construct three-dimensionally organized molecular architectures.

In this paper we report the formation of multilayered films of layered inorganic–organic nanocomposites derived from a series of alkylmethoxysilanes, containing various alkyl chain lengths and numbers of methoxy groups ($C_nH_{2n+1}(CH_3)_mSi(OMe)_{3-m}$, $m = 0-2$, $n = 8-12$), in the presence of tetramethoxysilane. This is the first report on the successful construction of sol–gel-derived organized nanostructures containing alkylmono- and alkylalkoxysilanes as the structural units. The characterization of the films and the role of tetramethoxysilane in the film formation are described in detail.

Experimental Section

Materials. n -Alkyltrimethoxysilanes ($C_nH_{2n+1}Si(OCH_3)_3$, C_nTMS , $n = 8, 10, \text{ and } 12$), n -alkylmethyldimethoxysilanes ($C_nH_{2n+1}Si(CH_3)(OCH_3)_2$, C_nMeDMS , $n = 8, 10, \text{ and } 12$), and n -alkyldimethylmethoxysilanes ($C_nH_{2n+1}Si(CH_3)_2(OCH_3)$, C_nMe_2MMS , $n = 8, 10, \text{ and } 12$) were synthesized by the methanolysis of the corresponding n -alkylchlorosilanes ($C_nH_{2n+1}Si(CH_3)_mCl_{3-m}$, $m = 0-2$, $n = 8-12$) purchased from Tokyo Kasei Co., except for n -dodecyltrichlorosilane and n -octyltrimethoxysilane, which were purchased from Chisso Co. The reactions of alkylchlorosilanes with absolute methanol (Kanto Chemical Co.) were performed at room temperature in the presence of pyridine (Kanto Chemical Co.), and the resulting products were vacuum distilled to afford clear liquids whose purities were checked by 1H , ^{13}C , and ^{29}Si NMR. Tetramethoxysilane (TMOS, Tokyo Kasei Co., > 98%) and tetrahydrofuran (Junsei Chemical Co.) were used for the film preparation without further purification. Deuterated THF (C_4D_8O ; THF- d_6 , Kanto Chemical Co.) was used as received in the NMR measurements.

Film Preparation. Precursor solutions were prepared by the cohydrolysis and polycondensation of alkylmethoxysilanes and TMOS in THF under acidic conditions. The molar compositions of the starting solutions were adjusted as follows: TMOS/alkylmethoxysilanes = 4, THF/Si = 4, $H_2O/OMe = 1$, and $HCl/Si = 0.0004, 0.002, \text{ and } 0.01$. The solutions stirred for 0.5, 1, 3, 6, 9, 12, and 24 h were spin-coated (3000 rpm, 10 s) on glass substrates. Every coating procedure was performed at around 25 °C and under a relative humidity of 30–45%.

The resulting gel films were dried at room temperature for 1 d so that further polycondensation proceeded.

Characterization. X-ray diffraction (XRD) patterns of the films were taken on a MAC Science M03XHF²² diffractometer using Mn-filtered Fe $K\alpha$ radiation. Solid-state ^{29}Si MAS NMR of the films was recorded on a JEOL JNM-CMX-400 spectrometer at a resonance frequency of 79.42 MHz with a 45° pulse and a recycle delay of 100 s. Thicker films were prepared by spin-coating at 500 rpm and then scratched from the substrates for the measurement. Field-emission (FE) scanning electron microscopy (SEM) images were obtained on a Hitachi S-4500S microscope at an accelerating voltage of 15 kV. For the FE-SEM measurements, Pt–Pd alloy was sputtered (6–12 nm in thickness) onto the cross-section of the cracked films. Transmission electron microscopy (TEM) images were recorded on a JEOL JEM-100CX microscope with an accelerating voltage of 100 kV. The films were scraped from the substrates and powdered for the TEM observations. Hydrolysis and polycondensation in the precursor solutions were monitored by liquid-state ^{29}Si NMR, and the spectra were recorded on a JEOL Lambda-500 spectrometer operating at 99.25 MHz. Sample solutions were put into 10 mm Teflon tubes, where THF- d_6 was mixed in the solvent (~10%) for obtaining lock signals and tetramethylsilane (TMS) was added for the internal reference. A small amount of $Cr(acac)_3$ (0.01 M) was dissolved for the relaxation of ^{29}Si nuclei. The measurements were performed at around 25 °C, and 64 scans were acquired with a recycle delay of 10 s. The solid-state and liquid-state ^{29}Si NMR spectra were measured with respect to tetramethylsilane.

Results and Discussion

Effect of the Reaction Conditions on Film Formation. The XRD patterns of the nanocomposite films derived from the C10TMS–, C10MeDMS–, and C10Me₂MMS–TMOS systems ($HCl/Si = 0.002$) are shown in Figures 1–3, respectively. The optical micrographs of the films obtained after the reactions for 1 and 3 h are also shown in the inset. The macroscopic homogeneity and the nanostructural ordering of the films depended largely on the reaction time in the precursor solutions. In all the systems, the solutions at the early stages of the reactions (0.5 and 1 h) afford inhomogeneous films with phase-separated morphologies. The films derived from the C10TMS– and C10MeDMS–TMOS systems showed XRD patterns typical of lamellar structures, whereas ordered films are not obtained from the C10Me₂MMS–TMOS system. As the reaction proceeded (~3 h), homogeneous and structurally ordered films, exhibiting sharp diffraction peaks at d spacings of 3.56, 3.67, and 4.06 nm, were obtained from the C10TMS–, C10MeDMS–, and C10Me₂MMS–TMOS systems, respectively. However, further reactions in the precursor solutions caused the gradual disordering of the nanostructures, and finally led to the formation of amorphous films (~24 h). Such a behavior is also described for film formation in the silica–surfactant sol–gel systems,¹⁵ and is associated with the degree of polycondensation in the precursor solutions. Thus, the controlled hydrolysis and polycondensation in the precursor solutions lead to the formation of well-ordered and transparent nanocomposite films.

(22) The environments of Si atoms in the silicate species formed by the hydrolysis and polycondensation processes are represented using the following notations: M^x ($x = 0-1$), D^x ($x = 0-2$), T^x ($x = 0-3$), and Q^x ($x = 0-4$) for alkylmono-, di-, and trimethoxysilane- and tetramethoxysilane-derived units, respectively, where x refers to the number of surrounding Si–O–Si bonds. If necessary, the number of remaining OH groups is shown as a subscript.

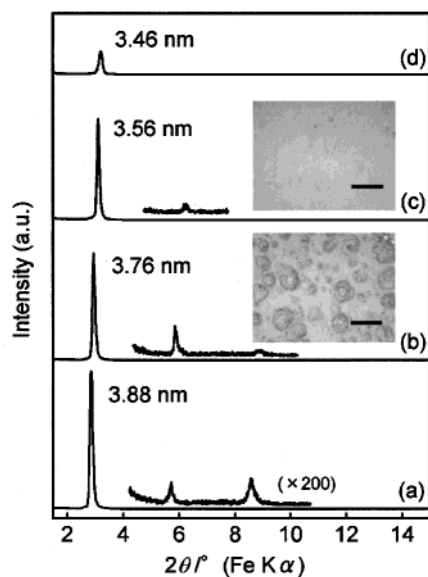


Figure 1. XRD patterns of the nanocomposite films prepared from the precursor solutions after the reactions for (a) 0.5 h, (b) 1 h, (c) 3 h, and (d) 6 h in the C10TMS–TMOS system (HCl/Si = 0.002). Inset: optical micrographs of the film surfaces for (b) and (c), scale bar 20 μm .

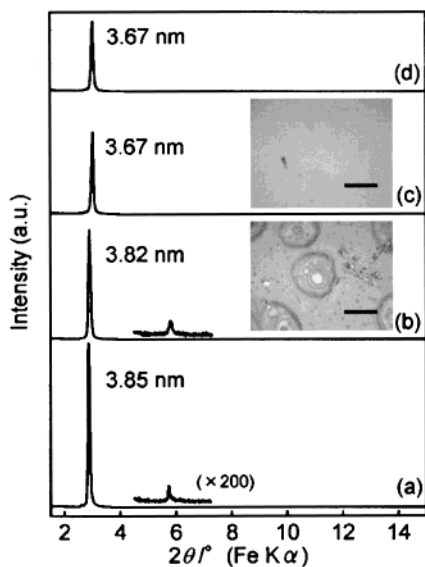


Figure 2. XRD patterns of the nanocomposite films prepared from the precursor solutions after the reactions for (a) 0.5 h, (b) 1 h, (c) 3 h, and (d) 6 h in the C10MeDMS–TMOS system (HCl/Si = 0.002). Inset: optical micrographs of the film surfaces for (b) and (c), scale bar 20 μm .

The TEM images of the ordered films prepared from the solution after reaction for 3 h are shown in Figure 4. Well-defined stripes due to the lamellar structures are observed, and the periodicities agree closely with the d spacings measured by XRD. The films derived from the C10MeDMS– and C10Me₂MMS–TMOS systems exhibit rather distorted structures compared to that derived from the C10TMS–TMOS system. The layered structures of these films were also confirmed by the structural collapse upon calcination at 450 °C for 6 h to remove organic constituents.

Figure 5 displays the ²⁹Si MAS NMR spectra for the films prepared from the solutions reacted for 3 h. The

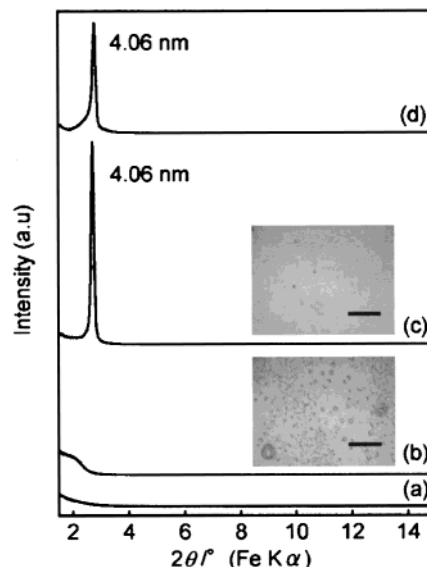


Figure 3. XRD patterns of the nanocomposite films prepared from the precursor solutions after the reactions for (a) 0.5 h, (b) 1 h, (c) 3 h, and (d) 6 h in the C10Me₂MMS–TMOS system (HCl/Si = 0.002). Inset: optical micrographs of the film surfaces for (b) and (c), scale bar 20 μm .

formation of siloxane networks derived from TMOS is confirmed in all the systems by the presence of the signals assigned to the Q² (−90 ppm), Q³ (−100 ppm), and Q⁴ (−110 ppm) environments of Si.²² In addition, the signals due to organosiloxane units derived from C10TMS, C10MeDMS, and C10Me₂MMS are observed at the T² (−55 ppm) and T³ (−65 ppm), D¹ (shouldered peak at −10 ppm) and D² (−16 ppm), and M¹ (13, 7 ppm) regions, respectively.²² The presence of unreacted Si–OH groups is confirmed for C10TMS- and C10MeDMS-derived units, while the C10Me₂MMS-derived units are fully reacted in the nanocomposite films. The evidence for co-condensation between alkylmethoxysilanes and TMOS was not obtained from the spectra of the C10TMS– and C10MeDMS–TMOS systems due to the broadness of the peaks (Figure 5a,b). In contrast, the signals due to the co-condensed species are clearly resolved in the C10Me₂MMS–TMOS system (Figure 5c). The small signal at ~7 ppm is assigned to a dimer (M¹–M¹ unit) on the basis of the liquid-state ²⁹Si NMR study for the hydrolysis and condensation of C_{*n*}Me₂–MMS. Consequently, the major signal at around 13 ppm is attributed to the co-condensed species between C_{*n*}Me₂–MMS and TMOS (M¹–Q^{*x*} unit).

The effect of the HCl/Si ratio in the starting solutions on film formation was examined. The optimum reaction time for the preparation of transparent and ordered films was different depending on the HCl/Si ratio in the precursor solutions. In the C10MeDMS–TMOS system, the formation of well-ordered films with good optical quality required a relatively longer reaction time (12 h) when HCl/Si = 0.0004, while only 1 h was needed with a much higher ratio of HCl/Si = 0.01. We confirmed that the ²⁹Si NMR spectrum of each reaction mixture exhibited an almost identical profile with that of the solution reacted for 3 h with HCl/Si = 0.002. Similar behavior was also observed for the C10TMS– and C10Me₂MMS–TMOS systems. It was also found that the films obtained at the earlier stages (0.5 and 1 h) were amorphous and less-ordered for the C10MeDMS–

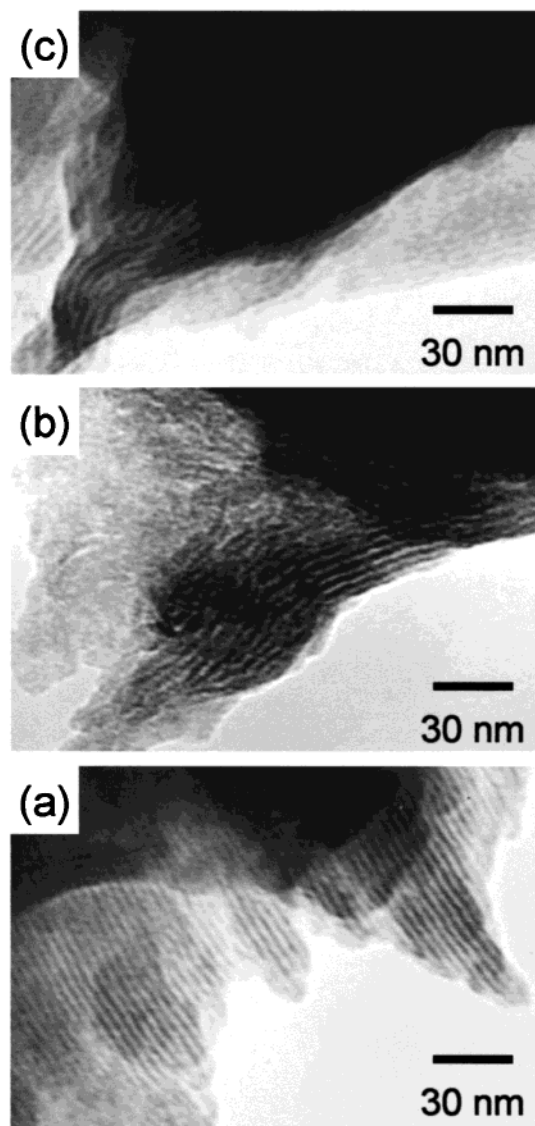


Figure 4. TEM images of the films derived from the (a) C10TMS–TMOS, (b) C10MeDMS–TMOS, and (c) C10Me₂MMS–TMOS systems (HCl/Si = 0.002, prepared after reaction for 3 h).

and C10TMS–TMOS systems, respectively, when HCl/Si = 0.0004. This tendency is consistent with that observed for the C10Me₂MMS–TMOS system when HCl/Si = 0.002 (Figure 3). These results again indicate that the nanostructural ordering of the films is mainly governed by the degree of polycondensation in the precursor solution.

Figure 6 compares the XRD patterns of the films derived from the C10MeDMS–TMOS system with different HCl/Si ratios in the starting solutions. The reaction time before the depositions was adjusted to 12, 3, and 1 h for HCl/Si = 0.0004, 0.002, and 0.01, respectively. All the films exhibit a similar *d*-spacing of ca. 3.7 nm ($2\theta = 3.0^\circ$), whereas the intensities of the diffraction peaks are drastically different. Such a difference in the peak intensities can be attributed either to the degree of structural order or to the orientational order of the stacked layers in the films because there was no substantial difference in the film thickness (ca. 1.0 μm). Figure 7 shows the SEM images for the cross-sections of the cracked films prepared with HCl/Si =

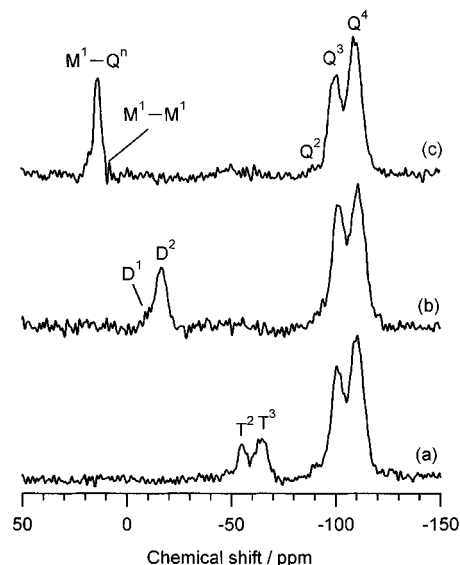


Figure 5. ²⁹Si MAS NMR spectra of the films derived from the (a) C10TMS–TMOS, (b) C10MeDMS–TMOS, and (c) C10Me₂MMS–TMOS systems (HCl/Si = 0.002, prepared after reaction for 3 h).

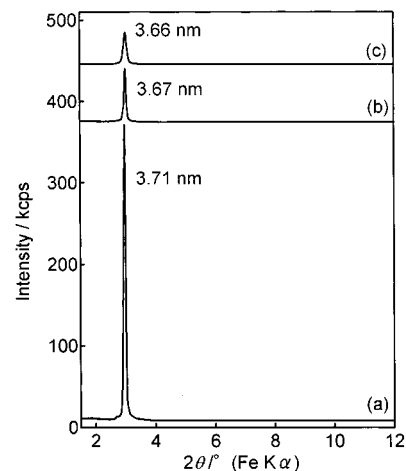


Figure 6. XRD patterns of the films prepared with different HCl/Si ratios of (a) 0.0004, (b) 0.002, and (c) 0.01 in the C10MeDMS–TMOS system (spin-coated after the reactions for 12, 3, and 1 h, respectively).

0.0004 and 0.002. Platelike morphologies with a thickness of 30–80 nm are clearly observed in both systems. Obviously these specific morphologies reflect the lamellar structure of the films. However, there is a large difference in the orientational order. The interior region of the film obtained with HCl/Si = 0.002 (Figure 7b) shows remarkably curved shapes of layered aggregates which are sandwiched by the oriented domains at narrow regions of the air–film and substrate–film interfaces. In contrast, the layers are entirely oriented parallel to the substrate surface in the film obtained with HCl/Si = 0.0004 (Figure 7a).

The variation of the HCl/Si ratio appears to have an effect not only on the hydrolysis and polycondensation in the precursor solutions but also on the subsequent gelation process.⁷ In the present system, preferential evaporation of the solvent during the spin-coating procedure induces the self-assembly of hydrolyzed alkylsiloxane oligomers, followed by gelation to form siloxane networks. The as-organized lamellar phase is simulta-

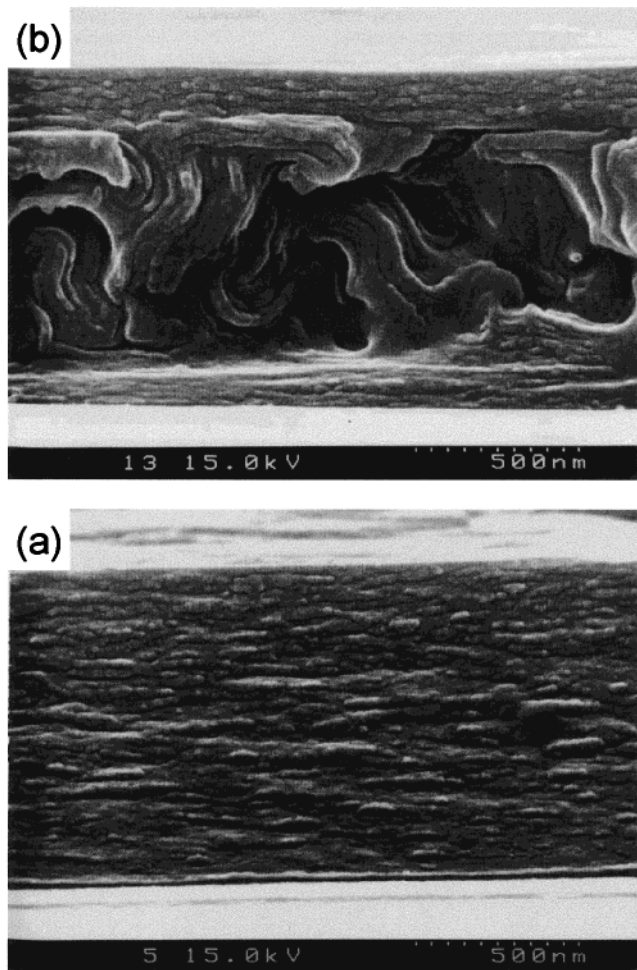


Figure 7. Cross-sectional SEM images of the films prepared with different HCl/Si ratios of (a) 0.0004 and (b) 0.002 in the C10MeDMS–TMOS system (spin-coated after the reactions for 12 and 3 h, respectively).

neously fixed by the polycondensation at higher HCl/Si ratios, while the lower HCl/Si ratios in the system may contribute to the gradual gelation that enables the rearrangement of the disoriented lamellar phase into well-oriented morphologies.

Similar nanocomposite films were prepared when the alkyl chain lengths in alkylmethoxysilanes were 8 and 12. The formation of ordered films required longer reaction times in the precursor solution with increasing chain length. In the $C_n\text{MeDMS}$ –TMOS systems (HCl/Si = 0.002), where $n = 8$ and 12, transparent and ordered films were obtained after the reactions for 1 and 6 h, respectively. This is ascribed in part to the difference in the condensation rate depending on the chain length. In this manner, the reaction time in the precursor solution was optimized depending on the number of methoxy groups and alkyl chain lengths. Figure 8 shows the relationship between the d values of the resulting nanocomposite films and the alkyl chain lengths of the alkylmethoxysilanes used. The d value increases continuously with increasing chain length and exhibits larger values as the number of methoxy groups decreases.

The conformation of the alkyl chains is examined by the peak positions of the CH_2 stretching vibrations ($\nu_{\text{as}}(\text{CH}_2)$ and $\nu_{\text{s}}(\text{CH}_2)$) in the IR spectra. These bands are observed at higher frequencies (2924 and 2854 cm^{-1} ,

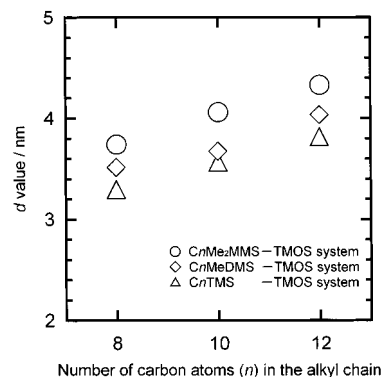


Figure 8. Relationship between the alkyl chain lengths (n) and the basal spacings (d) of the films.

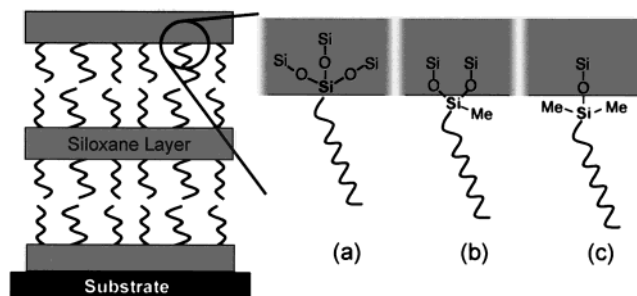


Figure 9. Proposed structural models for the inorganic–organic interfaces in the films derived from the (a) C10TMS–TMOS, (b) C10MeDMS–TMOS, and (c) C10Me₂MMS–TMOS systems.

respectively, for $n = 10$) than those of a crystalline state of long-chain amphiphiles (2918 and 2849 cm^{-1}),²³ indicating that the alkyl chains are not in an *all-trans* crystalline state. The arrangement of the alkyl chains in the interlayer spaces is assumed to be in either a monolayer or bilayer configuration based on the general representation of amphiphilic lamellar phases.²⁴ In these cases, the increases in the interlayer distances per one methylene carbon (CH_2) give the maximum values of 0.127 and 0.254 nm for the monolayer and bilayer, respectively, when the chains are in an *all-trans* conformation and are oriented normal to the siloxane layers. In Figure 8, the average increments in the d values per CH_2 for the films derived from the $C_n\text{TMS}$ –, $C_n\text{MeDMS}$ –, and $C_n\text{Me}_2\text{MMS}$ –TMOS systems are ca. 0.13, 0.13, and 0.15 nm, respectively. These values appear to be too large if the alkyl chains are arranged in a monolayer because the chains contain a substantial amount of gauche defects and are not in extended states. Therefore, it is likely that the alkyl chains are in bilayer arrangements.

From all the results described above, the structural models for the nanocomposite films are schematically illustrated in Figure 9. The films have multilayered structures consisting of a bilayer arrangement of alkyl chains that are covalently attached to siloxane layers. The observed difference in the d value with varying number of methoxy groups in the starting alkylmethoxysilanes (Figure 8) is probably attributed to the variation in the interfacial structures. It is supposed that the trialkoxysilyl groups are in part integrated into the

(23) Porter, M. D.; Bright, T. B.; Allara, D. L.; Chidsey, C. E. D. *J. Am. Chem. Soc.* **1987**, *109*, 3559.

(24) Tiddy, G. J. T. *Phys. Rep.* **1980**, *57*, 1.

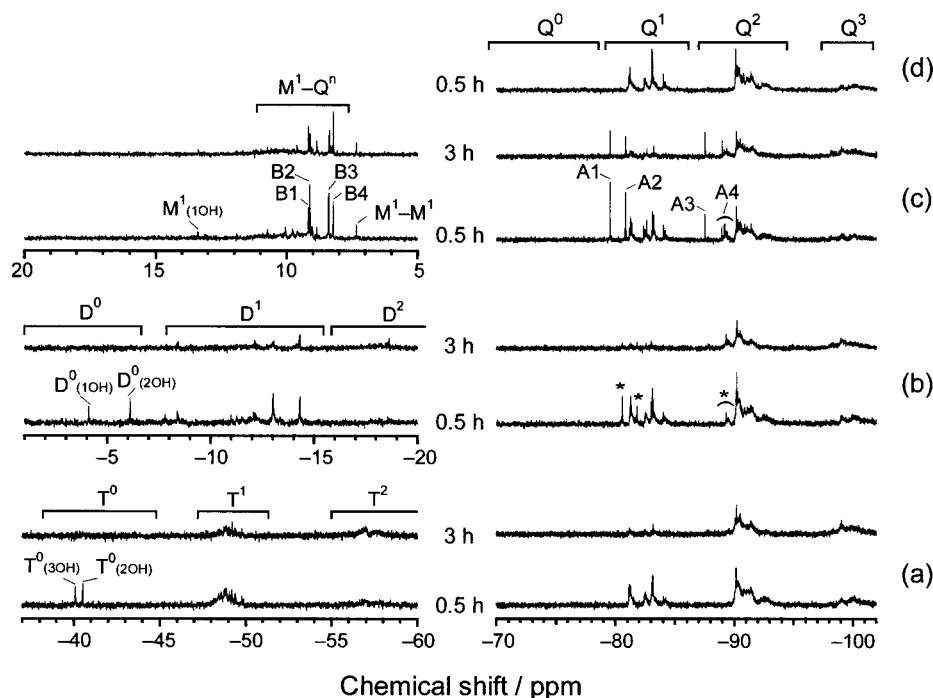


Figure 10. ^{29}Si NMR spectra of the precursor solutions in the (a) C10TMS–TMOS, (b) C10MeDMS–TMOS, and (c) C10Me₂MMS–TMOS systems after the reactions for 0.5 and 3 h. In addition, (d) shows the spectrum of the solution in which only TMOS was hydrolyzed for 0.5 h.

siloxane networks due to their cross-linking abilities, while the substitution of methyl groups for methoxy groups results in grafting on the external surface of silica layers.

Cohydrolysis and Polycondensation in the Precursor Solutions. To investigate the molecular species formed in the precursor solutions, cohydrolysis and polycondensation processes were followed by ^{29}Si NMR. Figure 10 shows the ^{29}Si NMR spectra of the precursor solutions in the C10TMS–, C10MeDMS–, and C10Me₂MMS–TMOS systems ($\text{HCl}/\text{Si} = 0.002$) after reaction for 0.5 and 3 h. The spectrum for the solution where only TMOS was hydrolyzed for 0.5 h is also shown in Figure 10d. In these systems, the signals due to the monomeric species derived from TMOS (Q^0) disappear in the initial reaction for 0.5 h, and various silicate species are present in the Q^1 , Q^2 , and Q^3 regions (no signals are detected in the Q^4 region). Although the small signals due to monomeric species of M, D, and T units are observed after 0.5 h, they completely disappear after 3 h.

Several reports on the cohydrolysis and polycondensation reactions in organoalkoxysilane–tetraalkoxysilane systems demonstrate the formation of co-condensed species at the initial stage of the reactions.^{25–30} In the C10TMS–TMOS system (Figure 10a), the spectra are so complicated, even after 0.5 h, that it is difficult to identify specific signals due to the co-condensed species.

However, it is likely that a substantial degree of co-condensation occurred, because such a high degree of condensation of T units was not observed when only C10TMS was reacted. On the other hand, in the C10MeDMS–TMOS system (Figure 10b), evidence for the co-condensation is provided by the appearance of new signals in the Q^1 and Q^2 regions (labeled with asterisks) that are not observed in Figure 10d. The detailed assignment of the signals is unsuccessful due to the structural diversity of the oligomeric species.

In the C10Me₂MMS–TMOS system, more detailed information can be obtained due to the lower cross-linking ability of monomethoxysilanes. As shown in Figure 10c, four signals labeled as A1, A2, A3, and A4 can be ascribed to co-condensed species (Q^1 – M^1 units) because these signals never appear in the spectrum of the solution containing only TMOS (Figure 10d). In addition, the small signals appearing at 13.4 and 7.3 ppm are assigned to a hydrolyzed monomer ($\text{M}^0_{(1\text{OH})}$)²² and dimer (M^1 – M^1), respectively, on the basis of the ^{29}Si NMR study for the hydrolysis and condensation of C10Me₂MMS. Accordingly, other signals detected at the M^1 region should be ascribed to the molecular species co-condensed with TMOS derived units (M^1 – Q^x units). From these results, the signals observed in the Q^1 region (A1 and A2) are assigned to M^1 – $\text{Q}^1_{(3\text{OH})}$ and M^1 – $\text{Q}^1_{(2\text{OH})}$,²² respectively, on the basis of the general findings that the signal due to tetraalkoxysilane is shifted downfield as the hydrolysis proceeds to form Si–OH groups.⁷ The signals at the M^1 region corresponding to these codimers are B2 and B3, because they exhibit intensities similar to those of the signals labeled as A1 and A2 during the reaction. These results indicate that the formation of co-condensed oligomers is predominant at the early stage of the reactions, while a relatively low degree of condensation occurs between alkylmethoxysilanes to form M^1 – M^1 units.

(25) Iwamoto, T.; Morita, K.; Mackenzie, J. D. *J. Non-Cryst. Solids* **1993**, *159*, 65.

(26) Babonneau, F.; Bois, L.; Livage, J. *Mater. Res. Soc. Symp. Proc.* **1992**, *271*, 237.

(27) Sugahara, Y.; Okada, S.; Kuroda, K.; Kato, C. *J. Non-Cryst. Solids* **1992**, *139*, 25.

(28) Sugahara, Y.; Inoue, T.; Kuroda, K. *J. Mater. Chem.* **1997**, *7*, 53.

(29) Delattre, L.; Babonneau, F. *Mater. Res. Soc. Symp. Proc.* **1994**, *346*, 365.

(30) Rodríguez, S. A.; Colón, L. A. *Chem. Mater.* **1999**, *11*, 754.

Role of TMOS in Self-Assembly. Hydrolysis and polycondensation of long-chain alkylalkoxysilanes normally result in the formation of phase-separated products,^{18,31} and homogeneous films cannot be obtained unless tetraalkoxysilane is added. Moreover, in the present system, co-condensation between alkylmethoxysilanes and TMOS in the precursor solution plays a crucial role in the formation of ordered nanocomposite films. This is supported by the fact that the films obtained at the early stages of the reactions in all three systems exhibit amorphous or less-ordered structures. In the precursor solutions that afford ordered and transparent films (e.g., after 3 h of reaction with HCl/Si = 0.002), monomeric species almost disappear and the oligomeric species including substantial amounts of co-condensed units are present (Figure 10). These results provide strong evidence that the origin of self-assembly in this system is quite different from that of the conventional single-component systems using alkyltrialkoxysilanes or alkyltrichlorosilanes alone.

In the sol-gel reactions of the alkylalkoxysilane-tetraalkoxysilane binary system, co-condensation rather than self-condensation of alkylmethoxysilanes should be dominant due to the steric repulsion between long alkyl chains and also the greater mobility of TMOS-derived species.^{29,30} Furthermore, under the presence of relatively large amounts of tetraalkoxysilane (TMOS/alkylmethoxysilane = 4), hydrolyzed alkylmethoxysilane molecules are much more likely to co-condense with TMOS-derived units. The alkylsiloxane oligomers thus formed can be regarded as amphiphilic molecules containing both hydrophobic alkyl chains and hydrophilic silanol groups. We suppose that the construction of ordered films relies on self-assembly of these oligomeric species by rapid evaporation of the miscible solvent during the spin-coating procedure.

In the case of the amphiphilic molecules containing an alkyl chain as the hydrophobic part and hydroxyl groups as the hydrophilic part, the ability to form liquid crystalline phases depends largely on the number of OH groups as well as the alkyl chain length.^{32,33} In the present system, the average number of Si-OH groups formed in the course of the reaction should become larger in the order $CnMe_2MMS < CnMeDMS < CnTMS$, not only in the monomeric state but also in the oligo-

meric state. For example, the number of OH groups for three different codimers (M^1-Q^1 , D^1-Q^1 , and T^1-Q^1) is 3, 4, and 5, respectively, provided that the methoxy groups are fully hydrolyzed. In addition, the co-condensation rate appears to be higher with the increase in the number of reactive methoxy groups. For these reasons, a longer reaction time was needed with the decrease in the number of methoxy groups. It is noteworthy that, in the $C10Me_2MMS$ -TMOS system (HCl/Si = 0.002), the ordered films were not obtained from the solution after reaction for 0.5 h despite the presence of various co-condensed species (Figure 10c). Comparing the two spectra for the solutions after 0.5 and 3 h, the signals at the Q^1 region observed after 0.5 h almost disappear after 3 h and Q^2 and Q^3 units are predominantly present. This result suggests that at least two Q units should be linked to one M unit ($M^1-Q^2-Q^x$ or $M^1-Q^3(-Q^x)_2$) for the formation of ordered nanocomposite films.

Conclusions

We have demonstrated a successful formation of novel alkylsiloxane multilayers by the cohydrolysis and polycondensation of a series of alkylmethoxysilanes, with various functionalities and alkyl chain lengths, in the presence of tetramethoxysilane. The present methodology is quite simple and effective, utilizing typical sol-gel reactions, by which the macroscopic homogeneity, nanostructural ordering, and orientation of the layers in the films were easily controlled. This is the first example of the construction of nanostructured materials by sol-gel reactions using mono- and difunctional organosilanes as the starting materials. It is evident that co-condensation between alkylmethoxysilane and tetramethoxysilane in the precursor solutions is essential for self-assembly into ordered nanocomposites. The extension to other systems utilizing various organoalkoxysilanes may lead to the production of novel layered nanocomposite films with covalently attached organic functionalities between silica layers.

Acknowledgment. We are grateful to Professor Y. Sugahara (Waseda University) for helpful discussions and also to Mr. T. Goto and Mr. H. Matsumoto (Material Characterization Central Laboratory, Waseda University) for FE-SEM and TEM measurements. This work is supported by a Grant-in-Aid for the Scientific Research by the Ministry of Education, Science, Sports, and Culture of the Japanese Government.

CM0101125

(31) Loy, D. A.; Baugher, B. M.; Baugher, C. R.; Schneider, D. A.; Rahimian, K. *Chem. Mater.* **2000**, *12*, 3624.

(32) Tschierske, C. *J. Mater. Chem.* **1998**, *8*, 1485.

(33) Goodby, J. W.; Mehl, G. H.; Saez, I. M.; Tuffin, R. P.; Mackenzie, G.; Auzély-Velty, R.; Benvegnu, T.; Plusquellec, D. *Chem. Commun.* **1998**, 2057.